DOI: 10.1002/ejic.200801052

Extended Members of the Layered Rare-Earth Hydroxide Family, $RE_2(OH)_5NO_3{\cdot}nH_2O$ (RE = Sm, Eu, and Gd): Synthesis and Anion-Exchange Behavior

Kyung-Hee Lee[a] and Song-Ho Byeon*[a]

Keywords: Rare earths / Ion exchange / Layered compounds / Host-guest systems / Intercalations

Three new layered rare-earth hydroxides (LRHs), $RE(OH)_{2.5}(NO_3)_{0.5}{\cdot}xH_2O$ (RE = Gd, Eu, and Sm), have been prepared by a hydrothermal reaction. These materials correspond to the extended members of the $RE_2(OH)_5NO_3{\cdot}nH_2O$ (RE = the rare-earth series) family. Although it has been suggested that the LRH structure seems to be kinetically favored by yttrium or (the second half of) the small rare-earth ions, an appropriate control of pH conditions for the hydrothermal reaction could extend this family to the larger rare-earth ions in the present study. The ion-exchange reactions between NO_3^- and diverse organic anions (a series of organic carboxylates, 1-alkanesulfonates, and alkylsulfates) were successfully carried out in the gallery of layered rare-earth hydroxides, $RE_2(OH)_5NO_3{\cdot}nH_2O$ (RE = Gd, Eu, and Sm). The FTIR spectra of the LRH hosts and some selected organic anion-exchanged derivatives clearly revealed the absence of nitrate and the appearance of characteristic bands attributed to carboxylate and sulfonate groups after the exchange reactions. Despite a large expansion of interlayer spacing, the layered gadolinium hydroxide and the long alkyl chain anion-exchanged derivative showed a similar paramagnetic behavior.

Introduction

Since the basic study on rare-earth hydroxy compounds containing the inorganic anions such as halides, nitrates, and carbonates[1] it has been accepted that the variables in the general formula could be $0.25 \leq m \leq 1.0$ and $0 \leq n \leq 1.0$ for the rare-earth hydroxysalts $RE(OH)_{3-m}X_m{\cdot}nH_2O$ (RE = rare-earths and X = inorganic anions). Although the phase equilibria and crystal structures of several $m = 1$ salts, $RE(OH)_2X$ and $RE(OH)_2X{\cdot}nH_2O$, have been investigated,[2] the members with $m \neq 1$ are still not well understood. For instance, $RE(OH)_{2.5}(NO_3)_{0.5}{\cdot}nH_2O$, $RE(OH)_{2.57}(NO_3)_{0.43}$, $RE(OH)_{2.69}(NO_3)_{0.31}$, $RE(OH)_{2.55}Cl_{0.45}$, $La(OH)_{2.57}I_{0.43}$, and $RE(OH)_{2.57}Br_{0.43}$ were reported but their crystal structures were suggested to be monoclinic, orthorhombic, or hexagonal, depending on the authors.[3] Nevertheless, the general structure of such a rare-earth hydroxide family is quite similar to that of layered double hydroxides (LDHs) consisting of alternating positively charged hydroxide and anion layers. It is well known that LDHs have attracted a great deal of interest because they have a number of attractive properties including heterogeneous catalysis, anion adsorption, anion exchange, as bioactive nanocomposites, and drug-delivery.[4] Because of a potential application of rare-earth complexes in optoelectronic devices,[5] the chelate complexes containing rare-earth ions such as La^{3+}, Eu^{3+}, and Gd^{3+} have also been incorporated in the galleries of LDHs.[6] In contrast, only a few studies have so far been directed to develop a synthetic method and to carry out a host-guest reaction for the layered materials composed of pure cationic rare-earth hydroxide layers (layered rare-earth hydroxides; LRHs).

The first anion-exchange reaction between the rare-earth hydroxocation layers, was carried out with $La(OH)_2NO_3{\cdot}H_2O$ and its interlayer chemistry was compared with those of classical LDHs.[7] However, it was not until very recently that new LRHs able to incorporate guest molecules in their interlayer spaces, $RE(OH)_{2.5}(A^{2-})_{0.25}{\cdot}H_2O$ or $[RE_4(OH)_{10}(H_2O)_4]A$ (RE = the second half of the rare-earths and A = 2,6-naphthalenedisulfonate and 2,6-anthraquinonedisulfonate) were reported.[8] The rare-earth atoms in the cationic layer of these materials occupy dodecahedral and a monocapped square antiprismatic site formed by the intralayer OH groups and the interlayer water molecules. These pillared LRHs showed a capability as heterogeneous catalysts in green chemistry. A family of $RE_2(OH)_5NO_3{\cdot}nH_2O$, which has a large ion-exchange capacity for a wide range of organic anions, was then synthesized under hydrothermal conditions.[9] It was suggested in those two previous works that the LRH structure seems to be kinetically favored by small rare-earth ions, with Gd^{3+} having a limiting cationic radius for these structures.

[a] College of Environment and Applied Chemistry, Kyung Hee University,
Yong-In, Kyung-Ki 446-701, Korea
Fax: +82-31-202-7337
E-mail: shbyun@khu.ac.kr

Supporting information for this article is available on the WWW under http://www.eurjic.org/ or from the author.

Because the hydrothermal reaction is quite sensitive to the temperature, pH, or aging conditions, we envisaged that an optimized synthesis condition could extend the LRH structure to the first half of the rare-earth series. Highly polarizable hydroxocation layers containing larger rare-earths would be expected to be more flexible for the exchange reaction with diverse organic and inorganic anions in the interlayer gallery. In this paper we report on the successful synthesis of RE = Sm, Eu, and Gd members of the $RE_2(OH)_5NO_3{\cdot}nH_2O$ family by using a hydrothermal reaction under a controlled pH condition.[10] Although the RE = Gd member has been reported as a mixed phase, its pure phase with improved crystallinity and host-guest reactivity could be prepared at a controlled pH range. A series of organic sulfonate, sulfate, and carboxylate anions are easily intercalated into these new layered rare-earth hydroxides by an ion-exchange reaction. Well-developed X-ray diffraction patterns of the obtained LRH-organic anion hybrids exhibit the typical and the classical host-guest reaction behavior, which is dependent on the chain length and tilting degree of the guest molecules.

Results and Discussion

Synthesis and Characterization of LRH Host Compounds (RE = Gd, Eu, and Sm)

The hydrothermal synthesis of the LRHs (layered gadolinium hydroxynitrate; LGdH, layered europium hydroxynitrate; LEuH, and layered samarium hydroxynitrate; LSmH) was sensitive to the pH conditions as expected. A careful adjustment around pH ≈ 6.7–7.2 was required for the formation of the layered hydroxide structure. Reactions at a higher pH range produced a considerable amount of $RE(OH)_3$ as an impurity phase. A low percentage yield of product was recovered at a lower pH range. In particular, the percentage yield of LSmH, which is prepared over a narrow pH range, was always limited to <30%. Despite extensive changes to pH, temperature, and aging conditions, we were unable to produce the phases of the larger rare-earths such as RE = La and Nd.

Powder X-ray diffraction (XRD) patterns of LGdH, LEuH, and LSmH are shown in Figure 1. A series of strong (00*l*) reflections is characteristic of a layered phase and corresponds to an interlayer separation of ca. 8.5 Å. As observed in the XRD patterns of previously reported $RE_2(OH)_5NO_3{\cdot}1.5H_2O$ (RE = Y, Tb–Tm) phases,[9] there are a number of very weak non-(00*l*) reflections, indicating that the layers are ordered. To confirm this order within the *ab* plane, the selected area electron diffraction (SAED) patterns were measured for the prepared materials. Well arranged spots shown in Figure 2 are quite similar to those of RE = Y, Tb–Tm members and confirm an order within the *ab* plane. Since, unfortunately, we were unsuccessful in obtaining single crystals of LGdH, LEuH, and LSmH, the lattice parameters were estimated from powder XRD and SAED patterns (a ≈ 7.3 Å, b ≈ 12.9 Å, c ≈ 17.1 Å, and β ≈ 92° of a monoclinic cell).

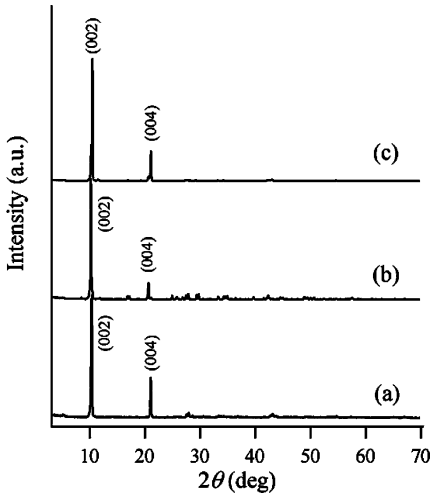

Figure 1. Powder X-ray diffraction patterns of (a) LGdH [$Gd_2(OH)_5NO_3{\cdot}H_2O$], (b) LEuH [$Eu_2(OH)_5NO_3{\cdot}H_2O$], and (c) LSmH [$Sm_2(OH)_5NO_3{\cdot}H_2O$].

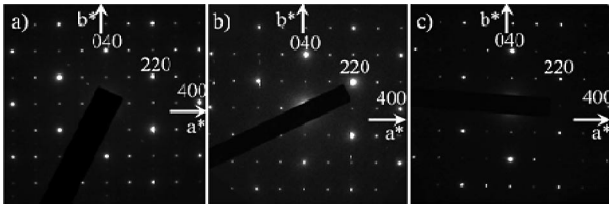

Figure 2. Selected area electron diffraction (SAED) patterns of (a) LGdH [$Gd_2(OH)_5NO_3{\cdot}H_2O$], (b) LEuH [$Eu_2(OH)_5NO_3{\cdot}H_2O$], and (c) LSmH [$Sm_2(OH)_5NO_3{\cdot}H_2O$].

The composition of LGdH, LEuH, and LSmH was determined to be $RE_2(OH)_5NO_3{\cdot}nH_2O$ (n ≈ 1.0) by inductively coupled plasma (ICP) and elemental analyses (EA). The proposed chemical formulae and observed interlayer spacings are summarized in Table 1. It was found that the amount of interlayer entrapped water is dependent on the synthetic conditions and influences on the interlayer spacing. For example, when dried at room temperature the amount of water in the interlayer increased to n ≈ 1.5. The resulting $RE_2(OH)_5NO_3{\cdot}1.5H_2O$ (RE = Gd, Eu, and Sm) exhibited an interlayer separation of ca. 9.2 Å, which is close to those of the RE = Y, Tb–Tm members.[9] The thermogravimetry (TG) curves for LGdH and LEuH [see Supporting Information Figures S1(a) and (b)] showed that the hydroxide decomposes at a temperature that is lower than and distinctly separated from that of the nitrate ion. In contrast, the thermal decompositions of hydroxide and nitrate are not well distinguished for LSmH [see Supporting Information Figure S1(c)]. If we consider that the ignition of three members above 650 °C yields RE_2O_3 (RE = Gd, Eu, and Eu) oxide, the observed total ignition loss of 24.2%, 24.6%, and 24.9% is close to the loss of 24.4%, 24.9%, and 25.1%, respectively, calculated from the composition of Table 1.

Table 1. Elemental analysis data of the layered rare-earth hydroxides, $RE_2(OH)_5NO_3{\cdot}nH_2O$.

Comp.	Composition	Elemental analysis [%] Obsd.	Calcd.	Basal spacing [Å]
LGdH	$Gd_2(OH)_5NO_3{\cdot}H_2O$	Gd 65.3	Gd 65.6	8.5
		N 2.5	N 2.9	
		H 1.5	H 1.5	
LEuH	$Eu_2(OH)_5NO_3{\cdot}H_2O$	Eu 65.2	Eu 64.8	8.6
		N 2.5	N 2.7	
		H 1.4	H 1.5	
LSmH	$Sm_2(OH)_5NO_3{\cdot}H_2O$	Sm 65.2	Sm 64.6	8.4
		N 2.8	N 3.0	
		H 1.3	H 1.5	

Organic Anion-Exchanged Hybrids of LRHs

Addition of a threefold excess of organic sulfates, sulfonates, or carboxylates to a suspension of $RE_2(OH)_5NO_3{\cdot}nH_2O$ (RE = Gd, Eu, and Sm) in water led to an easy exchange of the NO_3^- ions from the host and intercalation of organic anion guests. The complete replacement of NO_3^- by the organic anions was confirmed by the absence of characteristic reflections for the host lattice in corresponding powder XRD patterns and the absence of nitrogen in the elemental analyses (EA) of the products. It is noted that the exchange reactions with short alkyl chain anions such as butane and hexanesulfonates, octylsulfate, and terephthalate were relatively slow and accordingly such reactions were carried out at 60 °C. In contrast, the reactions with long alkyl chain anions were facile, occurring even at room temperature within a few hours. Such a preference of LRHs for long-chain length anions could be ascribed to an increase of hydrophobic interactions between the hydrocarbon chains. For instance, the semiquantitative analysis showed that the affinity of alkylsulfonates for LDHs increases by ca. 6 $kJ{\cdot}mol^{-1}$ per CH_2 group.[11]

The chemical compositions and interlayer spacings (as determined using XRD, EA, and TG analyses) for selected organic guest intercalates of LGdH, LEuH, and LSmH are summarized in Table 2. The elemental analysis data for all compounds prepared in this work are listed in Table S1, S2, and S3 (see Supporting Information). Similarly to that of the host materials, the amount of interlayer water was variable depending on the synthetic conditions. It is interesting that the EA and TG analysis data (Figure S2) for decanoate ($C_9H_{15}COO^-$) exchange derivatives of LGdH, LEuH, and LSmH showed a higher amount of carbon than was anticipated from the amount of decanoate needed to balance the charge of the layers. No change in the amount of decanoate was observed even after several repeated washings, implying a significant interaction between the excess decanoate units and the hydroxide matrix. Considering that the eight- and nine-coordinate rare-earth atoms are linked through μ_3-OH groups,[8] an exchange between the OH^- and decanoate anion would not be supposed. Because ICP analysis revealed no sodium content in decanoate exchange derivatives, the possibility of incorporation as decanoate sodium salt could also be excluded. It is accordingly postulated that the neutral decanoic acid might be incorporated in the interlayer space of LRHs when maintaining the charge neutrality. Because of strong lateral dispersion interactions between long chain alkyl ions, an inclusion exceeding the exchange capacity is often induced.[12] An intercalation of excess neutral phosphonic acid has also been observed in the LDH-phosphonates.[13] However, the reason for the absence of excess intercalation behavior for LRH-sulfonates or sulfates remains complicated and requires further studies.

Table 2. Elemental analysis data of selected organic anion-exchanged products of $RE_2(OH)_5NO_3{\cdot}nH_2O$ (RE = Gd, Eu, or Sm).

Compound	Elemental analysis [%] Obsd.	Calcd.	Basal spacing [Å]
$Gd_2(OH)_5(C_4H_9SO_3){\cdot}1.5H_2O$	C 7.8	C 8.5	15.4
	N 0.1	N 0.0	
	H 3.0	H 3.0	
$Gd_2(OH)_5(C_6H_{13}SO_3){\cdot}1.5H_2O$	C 12.2	C 12.1	17.9
	N 0.0	N 0.0	
	H 3.2	H 3.5	
$Gd_2(OH)_5(C_8H_{17}SO_3){\cdot}1.5H_2O$	C 14.3	C 15.5	20.2
	N 0.1	N 0.0	
	H 4.1	H 4.1	
$Gd_2(OH)_5(C_{10}H_{21}SO_3){\cdot}1.5H_2O$	C 18.0	C 18.8	23.5
	N 0.0	N 0.0	
	H 4.4	H 4.4	
$Eu_2(OH)_5(C_8H_{17}OSO_3){\cdot}1.5H_2O$	C 14.7	C 15.4	20.6
	N 0.2	N 0.0	
	H 3.5	H 4.0	
$Eu_2(OH)_5(C_{10}H_{21}OSO_3){\cdot}1.5H_2O$	C 19.1	C 18.4	22.7
	N 0.0	N 0.0	
	H 4.5	H 4.5	
$Eu_2(OH)_5(C_{12}H_{25}OSO_3){\cdot}1.5H_2O$	C 20.7	C 21.2	24.1
	N 0.0	N 0.0	
	H 4.5	H 4.9	
$Sm_2(OH)_5(C_{10}H_{21}SO_3){\cdot}1.5H_2O$	C 17.7	C 18.9	22.2
	N 0.0	N 0.0	
	H 4.4	H 4.6	
$Sm_2(OH)_5(C_{12}H_{25}C_6H_5SO_3){\cdot}1.5H_2O$	C 28.1	C 29.2	29.4
	N 0.0	N 0.0	
	H 4.8	H 5.1	
$Sm_2(OH)_5(C_{12}H_{25}OSO_3){\cdot}1.5H_2O$	C 20.9	C 21.3	23.9
	N 0.0	N 0.0	
	H 4.4	H 4.9	

Figures 3 and 4 show the XRD patterns of alkanesulfonate-exchanged derivatives of LGdH and LEuH, respectively. As expected for a layered material, all the XRD patterns show a series of intense basal (00*l*) reflections. The systematic shifts of the (00*l*) reflections toward lower diffraction angles with an increasing hydrocarbon chain length of the alkanesulfonates is a characteristic of organic anion intercalated LRHs. The arrangement mode of organic hydrocarbon chains in the interlayer is often different depending on the nature of hosts and functional groups.[14] In general, it is supposed that the hydrocarbon chains stand vertically or tilt at an angle with respect to the host layer so as to form an interdigitating monolayer, normal bilayer, or partly interpenetrating bilayers. For an all-*trans* chain the increment in alkyl chain length with every additional methylene unit is 1.26 Å. The variation in interlayer spacing with the number of methylene units is linear with a slope of 1.33 and 1.29 for LGdH-alkanesulfonate and LEuH-

alkanesulfonate, respectively (insets of Figures 3 and 4, respectively). The observed slopes could therefore be accounted for by a normal bilayer arrangement with the methylene chain tilted by an angle of around 32° and 31° with respect to the LGdH and LEuH layers, respectively. Such an arrangement is schematically illustrated in Figure 5 (a). In this model, the oxygen atoms of the sulfonate anions (SO_3^-) are not equivalent. If these three oxygen atoms are equivalent, they could be equally anchored to the hydroxide layer, as shown in Figure 5 (b). In such a model, the S–C bond is perpendicular to the hydroxide layer, with the hydrocarbon chain tilting at an angle of around 55°. Thus, a basal spacing of 15.5 Å for $Eu_2(OH)_5(C_4H_9SO_3)\cdot 1.5H_2O$ as an example is attributed to a bilayer arrangement with two SO_3^- groups linked to the adjacent layers of LEuH but with the hydrocarbon chains partly interpenetrating or overlapped. This bilayer model was proposed by several authors[14a,15] and adopted for the LDH-dodecylbenzenesulfonate[14c] and the LDH-dodecanesulfonate.[16]

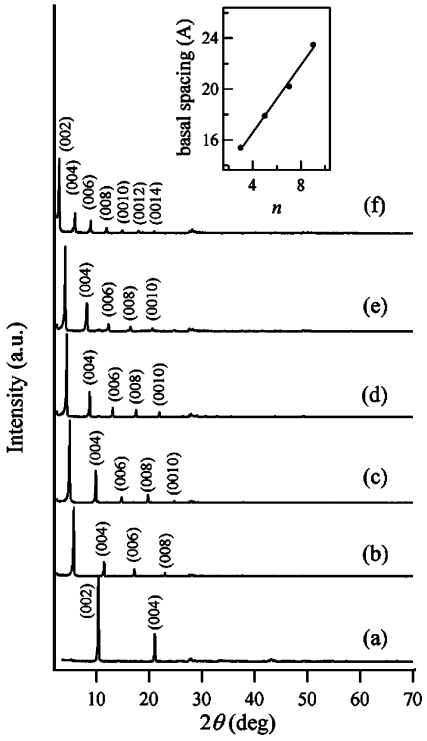

Figure 3. Comparison of XRD patterns of the (a) $Gd_2(OH)_5NO_3\cdot H_2O$ host and its (b) butanesulfonate, (c) hexanesulfonate, (d) octanesulfonate, (e) decanesulfonate, and (f) dodecylbenzenesulfonate exchanged compounds. The inset shows a plot of basal spacing vs. *n*, the number of methylene units in the alkyl chain.

Figures 6 and 7 show the XRD patterns of alkylsulfate-exchanged LGdH and LEuH, respectively. The basal spacing of samples depends on the length of the alkylsulfate hydrocarbon chain (Tables S1 and S2), demonstrating the incorporation of sulfate anions into the interlayer galleries of LRHs. The variation of interlayer separation as a function of the number of methylene units is linear with a slope

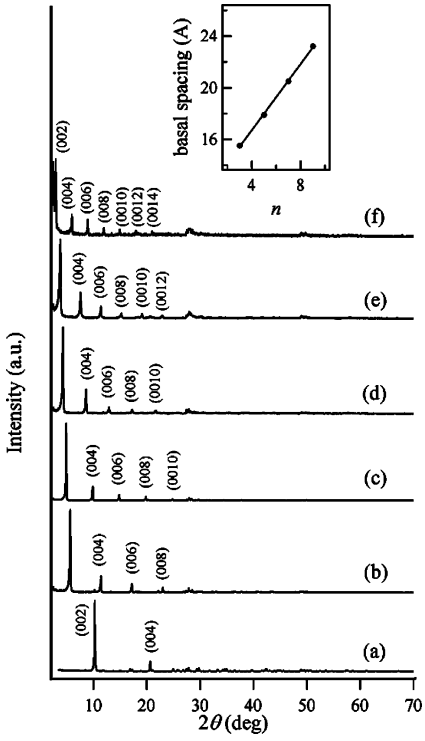

Figure 4. Comparison of XRD patterns of the (a) $Eu_2(OH)_5NO_3\cdot H_2O$ host and its (b) butanesulfonate, (c) hexanesulfonate, (d) octanesulfonate, (e) decanesulfonate, and (f) dodecylbenzenesulfonate exchanged compounds. The inset shows a plot of basal spacing vs. *n*, the number of methylene units in the alkyl chain.

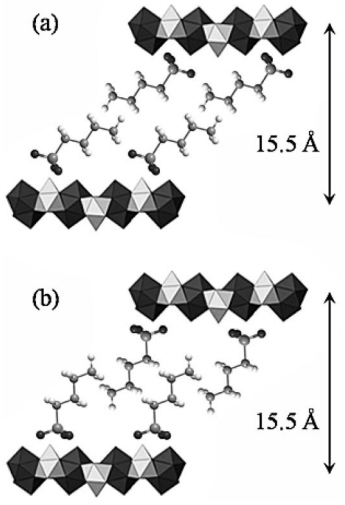

Figure 5. Two possible models representing (a) the tilted bilayer and (b) the interpenetrating bilayer arrangement of alkyl chains in the alkanesulfonate of the LRH. The interlayer arrangement of organic anions for $Eu_2(OH)_5(C_4H_9SO_3)\cdot 1.5H_2O$ is represented as an example. The structure model of ref.[8] was adopted for the hydroxocation layers.

of 0.93 and 0.88 for LGdH-alkylsulfate and LEuH-alkylsulfate, respectively (see insets of Figures 6 and 7). Compared with the linear intercarbon distance along the chain of 1.26 Å, these slopes could be ascribed to the formation of monolayers tilted by an angle of around 48° and 44° with

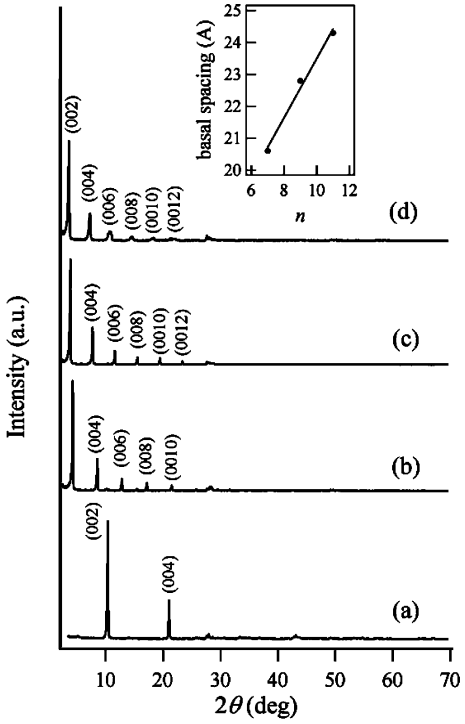

Figure 6. Comparison of XRD patterns of the (a) $Gd_2(OH)_5NO_3 \cdot H_2O$ host and its (b) octylsulfate, (c) decylsulfate, and (d) dodecylsulfate exchanged compounds. The inset shows a plot of basal spacing vs. *n*, the number of methylene units in the alkyl chain.

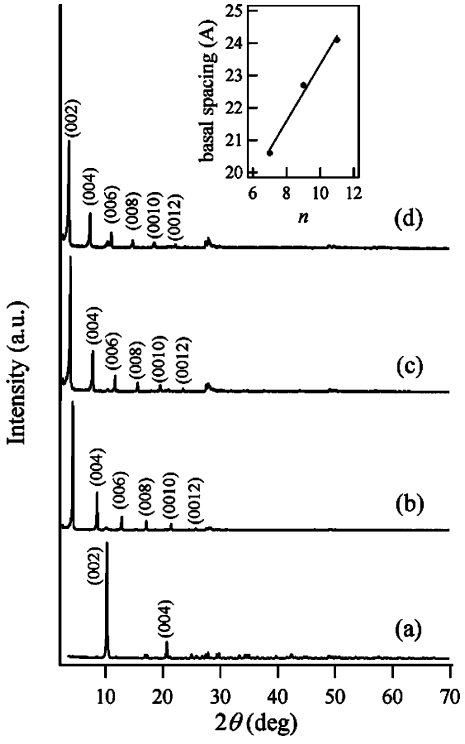

Figure 7. Comparison of XRD patterns of the (a) $Eu_2(OH)_5NO_3 \cdot H_2O$ host and its (b) octylsulfate, (c) decylsulfate, and (d) dodecylsulfate exchanged compounds. The inset shows a plot of basal spacing vs. *n*, the number of methylene units in the alkyl chain.

respect to LGdH and LEuH layers, respectively. In Figure 8, a schematic model for such an arrangement in $Eu_2(OH)_5(C_8H_{17}OSO_3) \cdot 1.5H_2O$ is illustrated as an example.

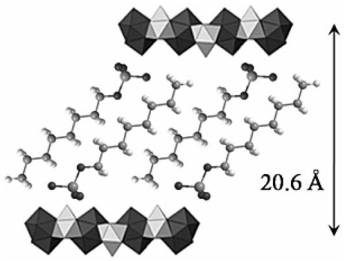

Figure 8. Model representing the tilted monolayer arrangement of alkyl chains in the LRH alkylsulfate. The interlayer arrangement of organic anions for $Eu_2(OH)_5(C_8H_{17}OSO_3) \cdot 1.5H_2O$ is represented as an example. The structure model of ref.[8] was adopted for the hydroxocation layers.

Figure 9 and Figure 10 show the XRD patterns of carboxylate-exchanged LGdH and LEuH, respectively. Well-developed (00*l*) reflections demonstrate again an excellent ion-exchange capacity between nitrate anion and organic carboxylate or dicarboxylate groups in the galleries of the LRHs. The interlayer separations of 13.4 and 13.1 Å for terephthalate [p-$C_6H_4(COO^-)_2$] intercalated LGdH and LEuH, respectively, are in agreement with that (13.1 Å) of the RE = Er member.[9] In contrast, the interlayer separation of 29.9 Å for decanoate ($C_9H_{15}COO^-$) derivatives of LGdH and LEuH is too large to be accounted for by a monolayer arrangement of anions between the layers. Considering the incorporation of excess neutral decanoic acid (Tables S1 and S2), it is possible to infer the formation of a normal tilted bilayer of anions in the interlayer gallery.

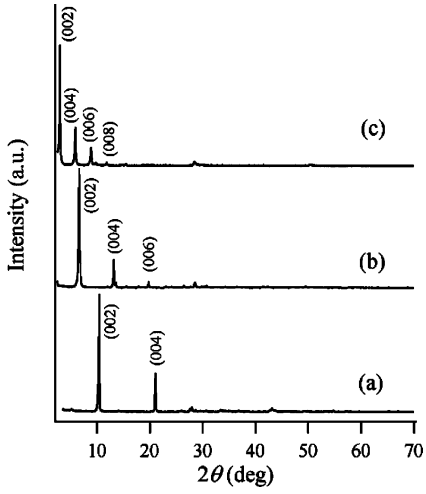

Figure 9. Comparison of XRD patterns of the (a) $Gd_2(OH)_5NO_3 \cdot H_2O$ host and its (b) terephthalate and (c) decanoate exchanged compounds.

All of the anion-exchange behaviors described for LGdH and LEuH derivatives are consistently observed with LSmH derivatives. As shown in Figure 11, the $Sm_2(OH)_5NO_3 \cdot nH_2O$ host also reveals an excellent ion-exchange reactivity for the organic sulfonates, sulfates, and carboxylates, dis-

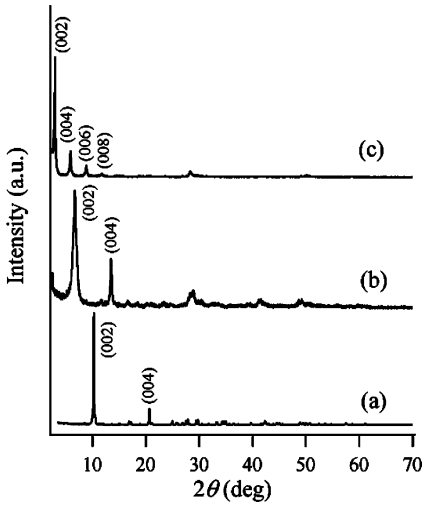

Figure 10. Comparison of XRD patterns of the (a) $Eu_2(OH)_5NO_3 \cdot H_2O$ host and its (b) terephthalate and (c) decanoate exchanged compounds.

playing the classical characteristic of a layered structure whose interlayer spacing strongly depends on the orientation of guest anions in the interlayer. On the basis of the observed expansion of interlayer spacings (Table S3), it could be proposed that the dodecylsulfate ($C_{12}H_{25}OSO_3^-$) and decanoate ($C_9H_{15}COO^-$) anions are packed in the manner of a tilted monolayer and bilayer in the interlayer gallery, respectively. In particular, an excess intercalation of neutral decanoic acid would facilitate a bilayer arrangement through an effective lateral hydrophobic interaction. Two possible modes, a tilted bilayer or an interpenetrating bi-

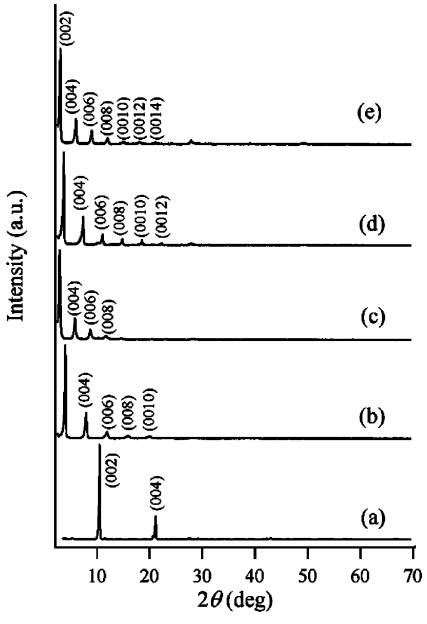

Figure 11. Comparison of XRD patterns of the (a) $Sm_2(OH)_5NO_3 \cdot H_2O$ host and its (b) decanesulfonate, (c) decanoate, (d) dodecylsulfate, and (e) dodecylbenzenesulfonate exchanged compounds.

layer packing of the hydrocarbon chains, could also be put forward for decanesulfonate ($C_{10}H_{21}SO_3^-$) and dodecylbenzenesulfonate ($C_{12}H_{25}C_6H_5SO_3^-$) derivatives.

FTIR Spectra

The FTIR spectra of LRH hosts are compared with those of some selected organic anion-exchanged derivatives in Figure 12. An intense and broad band centered at around 3450 cm^{-1} for all compounds is attributed to the stretching vibration of the hydroxyl group from both the hydroxide layers and the interlayer water.[17] A band at around 1635 cm^{-1} is assigned to the bending mode of water molecules. The intense band at 1384 cm^{-1} in the spectra of the LGdH, LEuH, and LSmH hosts, shown in parts (a), (b), and (c) of Figure 12 corresponds to the ν_3 mode of the nitrate species.[18] After exchange reactions of LGdH with terephthalate [p-$C_6H_4(COO^-)_2$] and LEuH with decanoate ($C_9H_{15}COO^-$) this ν_3 vibration is no longer detected, confirming the absence of NO_3^-. Instead, there are two intense bands observed at around 1553 and 1338 cm^{-1} for LGdH-terephthalate; see Figure 12 (a-1) and at around 1543 and 1455 cm^{-1} for LEuH-decanoate; Figure 12 (b-1)]. These two bands are assigned to $\nu_{as}(COO^-)$ and $\nu_s(COO^-)$, respectively. The difference between ν_{as} and ν_s (Δ = 165 cm^{-1}) for LGdH-terephthalate, which is larger than that (Δ = 88 cm^{-1}) for LEuH-decanoate, indicates that the dicarboxylate ion is in a pillared-arrangement mode.[18b]

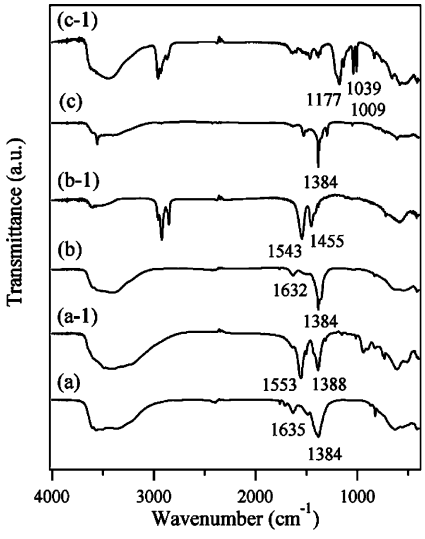

Figure 12. FTIR spectra of (a) $Gd_2(OH)_5NO_3 \cdot H_2O$, (a-1) $Gd_2(OH)_5$-(terephthalate)$_{0.5} \cdot 1.5H_2O$, (b) $Eu_2(OH)_5NO_3 \cdot H_2O$, (b-1) $Eu_2(OH)_5$-(decanoate)$\cdot 1.5H_2O$, (c) $Sm_2(OH)_5NO_3 \cdot H_2O$, and (c-1) $Gd_2(OH)_5$-(dodecylbenzenesulfonate)$\cdot 1.5H_2O$.

The bands observed at 2851 and 2922 cm^{-1} and at 2870 and 2958 cm^{-1} in Figure 12 (see parts b-1 and c-1) are assigned to the methylene symmetric and antisymmetric stretching modes of the alkyl chains of the intercalated organic anions.[19] In the IR spectrum of LSmH-dodecylbenzenesulfonate, see Figure 12 (c–1), a broad band at around 1177 cm^{-1} corresponds to $\nu_{as}(SO_3^-)$ and a sharp band at

1039 cm^{-1} is attributed to $\nu_s(SO_3^-)$.[12,20] Coupled with the observation of characteristic bands for the sulfonate group, the disappearance of the nitrate absorption peak around 1384 cm^{-1} confirms a complete exchange reaction.

Magnetic Properties of LGdH-NO_3 and LGdH-decanesulfonate

Variation of the magnetic moment versus temperature was recorded for the $Gd_2(OH)_5NO_3{\cdot}H_2O$ host and $Gd_2(OH)_5$(decanesulfonate)$\cdot 1.5H_2O$ derivative after zero-field cooling under an applied magnetic field of 0.5 T. The inverse magnetic susceptibility data of two compounds are compared as a function of temperature in Figure 13. No magnetic interaction is observed with both compounds in the measured temperature range (10–300 K). Instead, the magnetic properties of these members show pure paramagnetic behavior and obey a Curie–Weiss law. Observed effective magnetic moments of 7.58 and 7.72 μ_B/Gd for $Gd_2(OH)_5NO_3{\cdot}H_2O$ and $Gd_2(OH)_5(C_{10}H_{21}SO_3){\cdot}1.5H_2O$, respectively, are comparable with the theoretical spin-only value of 7.94 μ_B for Gd^{3+}. Considering a variable amount of interlayer water in both compounds, such an agreement of effective magnetic moments would support the proposed chemical compositions for these materials within experimental errors. No significant difference in the magnetic moment values between the LGdH host and long-chain alkylsulfonate-intercalated derivative indicates that the pure paramagnetic property of the f-orbital electrons in the hydroxide layer is not affected by a change in the interlayer environment.

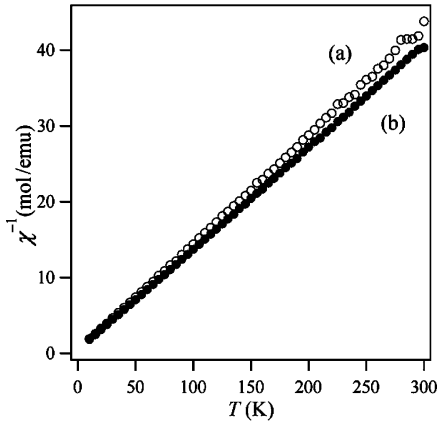

Figure 13. Inverse molar magnetic susceptibilities of (a) $Gd_2(OH)_5NO_3{\cdot}H_2O$ (μ_{eff} = 7.58) and (b) $Gd_2(OH)_5$(decanesulfonate)$\cdot 1.5H_2O$ (μ_{eff} = 7.72) as a function of temperature.

Conclusions

We have successfully synthesized three layered rare-earth hydroxides (LRHs), $RE_2(OH)_5NO_3{\cdot}nH_2O$ (RE = Gd, Eu, Sm; n = 1.0–1.5). Although it has been proposed that the cation size for this phase be limited to small rare-earths, these new materials prepared in the present work provide evidence that a controlled pH condition during hydrothermal synthesis can extend the members of the $RE_2(OH)_5NO_3{\cdot}nH_2O$ (RE = the rare-earth series) family to the larger rare-earth cations.

Highly polarizable hydroxocation layers enable these materials to undergo well-defined ion-exchange reactions with a wide range of organic anions. Similarly to the classical LDHs, the organophyllic nature of the LRH's interlayer space with surfactants as interlayer anions make them suitable materials for the adsorption of other organic molecules. These kinds of materials can also be used as catalysts, catalyst precursors, and (porous or ultrathin film) luminescent hosts after calcination at different temperatures. Therefore, new members of layered hydroxide-containing large rare-earth cations could contribute to widen the application range of the rare-earth materials.

Experimental Section

Synthesis of Layered Rare-Earth Hydroxides (LRHs): Layered gadolinium hydroxynitrate [$Gd_2(OH)_5NO_3{\cdot}nH_2O$; LGdH], layered europium hydroxynitrate [$Eu_2(OH)_5NO_3{\cdot}nH_2O$; LEuH], and layered samarium hydroxynitrate [$Sm_2(OH)_5NO_3{\cdot}nH_2O$; LSmH] were synthesized via a hydrothermal reaction. Typically, about 1.5 g of RE_2O_3 (RE = Gd, Eu, and Sm) was dissolved in 10% HNO_3 solution (40 mL). After clear solution was formed by uniform stirring, an aqueous KOH (10%) solution was added dropwise until the pH of the solution was adjusted to ca. 7.0, ca. 6.8, and ca. 6.7 at 30 °C for RE = Gd, Eu, and Sm, respectively. The resulting colloidal mixture was put into a Teflon-lined stainless steel autoclave with a capacity of 100 mL at room temperature. The autoclave was then sealed and maintained at 150–170 °C for 12 h. The solution was continuously stirred during the hydrothermal treatment. After the reaction was completed the solid product was collected by filtration, washed with distilled water, and dried at 40 °C for a day.

Anion-Exchange Reaction of LRHs: Intercalation of diverse organic anions was achieved using the ion-exchange method. In a typical reaction, the LRH powders (0.25 g) were dispersed into an aqueous anionic solution containing a threefold molar excess of a series of organic carboxylate, 1-alkanesulfonate, and alkylsulfate sodium salts. The ion-exchange reactions between NO_3^- and the organic anions were carried out at 60 °C (for butane and hexanesulfonates, octylsulfate, and terephthalate) or at room temperature (for other organic anions) for 1–10 h in air while stirring. Resulting precipitates were recovered by filtration, washed with water, and dried at 40 °C for a day.

Characterizations: The powder X-ray diffraction pattern was recorded with a rotating anode installed diffractometer (MacScience Model M18XHF). The Cu-K_α radiation used was monochromated by curved-crystal graphite. Field emission scanning electron microscopy (FE-SEM) was carried out with a Carl Zeiss LEO SUPRA electron microscope operating at 30 kV. Specimens that were investigated with the electron microscope were coated with Pt-Rh for 180 s under vacuum. Transmission electron microscopy (TEM) and selected area electron diffraction (SAED) observations were made with a JEOL JEM-2100F electron microscope operating at 300 kV. The composition of prepared compounds was determined by elemental analysis (CE Instruments Flash EA1112), thermogravimetry (Seiko Instruments TG/DTA320), and inductively coupled plasma (Thermo Elemental Thermo ICAP 6000) analysis. DC mag-

netic susceptibility measurements for selected sample powders were carried out over the temperature range 10 K to 300 K in an applied magnetic field of 0.5 T using a Quantum Design MPMS XL 7.0 magnetometer. Fourier transform infrared (FTIR) spectra, over a range of 400–4000 cm^{-1}, were measured with a JASCO FT/IR-4200 infrared spectrophotometer using the KBr pellet technique. A nominal resolution was 4 cm^{-1}.

Supporting Information (see also the footnote on the first page of this article): Thermogravimetry (TG) curves (Figures S1 and S2), SEM images (Figure S3), and elemental (CHN) analysis data for the LRHs and organic anion exchanged derivatives (Tables S1, S2, and S3).

Acknowledgments

This research was supported by the Korea Science and Engineering Foundation (KOSEF) through grant R01-2008-000-10442-0.

[1] a) R. F. Klevtsova, P. W. Klevtsova, *J. Struct. Chem.* **1966**, *7*, 524; b) F. L. Carter, S. Levinson, *Inorg. Chem.* **1969**, *8*, 2788; c) J. M. Haschke, L. Eyring, *Inorg. Chem.* **1971**, *10*, 2267; d) J. M. Haschke, *J. Solid State Chem.* **1975**, *12*, 115.

[2] a) M. Lundberg, A. Skarnulis, *Acta Crystallogr., Sect. B* **1976**, *32*, 2944; b) D. F. Mullica, E. L. Sappenfield, D. A. Grossie, *J. Solid State Chem.* **1986**, *63*, 231; c) D. Louer, M. Louer, *J. Solid State Chem.* **1987**, *68*, 292; d) T. Nilges, *Z. Naturforsch.* **2006**, *61b*, 117.

[3] a) J. M. Haschke, *Inorg. Chem.* **1974**, *13*, 1812; b) C. E. Holcomb, *J. Am. Ceram. Soc.* **1978**, *61*, 481; c) E. T. Lance-Gomez, J. M. Haschke, *J. Solid State Chem.* **1978**, *23*, 275; d) E. T. Lance, J. M. Haschke, *J. Solid State Chem.* **1976**, *17*, 55; e) E. T. Lance-Gomez, J. M. Haschke, W. Butler, D. R. Peacor, *Acta Crystallogr., Sect. B* **1978**, *34*, 758.

[4] a) P. S. Braterman, Z. P. Xu, F. Yarberry, *Handbook of Layered Materials*, Marcel Dekker, New York, **2004**; b) A. I. Khan, D. O'Hare, *J. Mater. Chem.* **2002**, *12*, 3191; c) B. F. Sels, D. E. De Vos, M. Buntinx, P. A. Jacobs, *J. Catal.* **2003**, *216*, 288; d) M. B. J. Roeffaers, B. F. Sels, H. Uji-i, F. C. De Schryver, P. A. Jacobs, D. E. De Vos, J. Hofkens, *Nature* **2006**, *439*, 572; e) Z. An, W. H. Zhang, H. M. Shi, J. He, *J. Catal.* **2006**, *241*, 319; f) H. Chen, F. Zhang, S. Fu, X. Duan, *Adv. Mater.* **2006**, *18*, 3089; g) J. Liu, R. Ma, M. Osada, N. Iyi, Y. Ebina, K. Takata, T. Sasaki, *J. Am. Chem. Soc.* **2006**, *128*, 4872; h) B. F. Sels, D. E. De Vos, P. A. Jacobs, *J. Am. Chem. Soc.* **2007**, *129*, 6916; i) Z. Gu, A. C. Thomas, Z. P. Xu, J. H. Campbell, G. Q. Lu, *Chem. Mater.* **2008**, *20*, 3715.

[5] a) H. Maas, A. Currao, G. Calzaferri, *Angew. Chem. Int. Ed.* **2002**, *41*, 2495; b) D. Sendor, U. Kynast, *Adv. Mater.* **2002**, *14*, 1570; c) H. R. Li, J. Lin, H. J. Zhang, L. S. Fu, Q. G. Meng, S. B. Wang, *Chem. Mater.* **2002**, *14*, 3651; d) E. Brunet, M. J. de la Mata, O. Juanes, J. C. Rodriguez-Ubis, *Chem. Mater.* **2004**, *16*, 1517.

[6] a) M. Kaneyoshi, W. Jones, *Mol. Cryst. Liq. Cryst.* **2001**, *356*, 459; b) C. Li, G. Wang, D. G. Evans, X. Duan, *J. Solid State Chem.* **2004**, *177*, 4569; c) S. Gago, M. Pillinger, R. A. SaFerreira, L. D. Carlos, T. M. Santos, I. S. Goncalves, *Chem. Mater.* **2005**, *17*, 5803.

[7] S. P. Newman, W. Jones, *J. Solid State Chem.* **1999**, *148*, 29.

[8] F. Gandara, J. Perles, N. Snejko, M. Iglesias, B. Gomez-Lor, E. Gutierrez-Puebla, M. Angeles Monge, *Angew. Chem. Int. Ed.* **2006**, *45*, 7998.

[9] L. J. McIntyre, L. K. Jackson, A. M. Fogg, *Chem. Mater.* **2008**, *20*, 335.

[10] At the end of this work the synthesis of some rare-earth hydroxychloride analogues was reported, F. Geng, H. Xin, Y. Matsushita, R. Ma, M. Tanaka, F. Izumi, N. Iyi, T. Sasaki, *Chem. Eur. J.* **2008**, *14*, 9255.

[11] Z. P. Xu, P. S. Braterman, *J. Phys. Chem. C* **2007**, *111*, 4021.

[12] R. Trujillano, M. J. Holgado, F. Pigazo, V. Rives, *Phys. B* **2006**, *373*, 267.

[13] G. R. Williams, D. O'Hare, *Solid State Sci.* **2006**, *8*, 971.

[14] a) M. Meyn, K. Beneke, G. Lagaly, *Inorg. Chem.* **1990**, *29*, 5201; b) S. Carlino, *Solid State Ionics* **1997**, *98*, 73; c) Z. P. Xu, P. S. Braterman, *J. Mater. Chem.* **2003**, *13*, 268.

[15] H. P. Boehm, J. Steinle, C. Vieweger, *Angew. Chem. Int. Ed. Engl.* **1977**, *16*, 265.

[16] B. Li, J. He, *J. Phys. Chem. C* **2008**, *112*, 10909.

[17] F. M. Labajos, V. Rives, M. A. Ulibarri, *J. Mater. Sci.* **1992**, *27*, 1546.

[18] a) K. Nakamoto, *Infrared and Raman Spectra of Inorganic and Coordination Compounds*, *4th ed.*, John Wiley & Sons, New York, **1986**; b) H. C. Zeng, Z. P. Xu, M. Qian, *Chem. Mater.* **1998**, *10*, 2277.

[19] R. A. MacPhail, H. L. Strauss, R. G. Snyder, C. A. Elliger, *J. Phys. Chem.* **1984**, *88*, 334.

[20] R. Trujillano, M. J. Holgado, J. L. Gonzalez, V. Rives, *Solid State Sci.* **2005**, *7*, 931.

Received: October 27, 2008
Published Online: January 28, 2009

